A Variational Approach for Optimal Diffusivity Identification in Firns

Emmanuel WITRANT[1] and Patricia MARTINERIE[2], April 30, 2010*

Abstract

Trace gas measurements in interstitial air from polar firn allow to reconstruct their atmospheric concentration time trends over the last 50 to 100 years. This provides a unique way to reconstruct the recent anthropogenic impact on atmospheric composition. Converting depth- concentration profiles in firn into atmospheric concentration histories requires models of trace gas transport in firn. A fundamental parameter of these models is firn diffusivity. Here we propose a new method to evaluate the diffusivity of polar firns using automatic control analysis techniques. More precisely, the diffusivity identification is formulated as an optimization problem in terms of partial differential equations (PDE). The proposed theorems generally apply to transport phenomena in non-homogeneous media (space-dependent coefficients), a variational approach is proposed and the optimization problem is solved with an adjoint-based gradient-descent algorithm.

1. Introduction

Polar ice cores provide a unique archive of atmospheric composition at time scales covering glacial-interglacial cycles (the last 800 000 years) to the rise of anthropogenic pollution (since about 1850 A.D.), as described in [1, 2] and references therein. Firn air pumping campaigns multiplied over the last decade for to major reasons: (1) large amounts of air can be retrieved, providing the opportunity to measure numerous trace gases [3], (2) direct observation of air trapping in ice provide information about the age difference between the air bubbles and the surounding ice, which should be well constrained in order to finely interpret ice core signals [4].

In polar regions where no melting occurs, snow transforms into ice through the effect of its own weight. The transition between an open-porosity material (snow/firn) into an airtight material (ice) then occurs at about 50-100 meters depth, as depicted in Figure 1. Within snow and firn (i.e. compacted snow), atmospheric trace gases are mostly transported by diffusion through air channels. Air trapping in bubbles also generates an advection flux which is most important at sites undergoing high snow accumulation rates. Finally gravitational fractionation occurs, transporting heavy molecules downward more efficiently. This slight fractionation needs to be taken into account at least for isotopic ratios, measured at the per-mil precision level. Such phenomena lead to the modeling of firns as non-homogeneous media where the trace gases move according to transport equations with space-dependent coefficients.

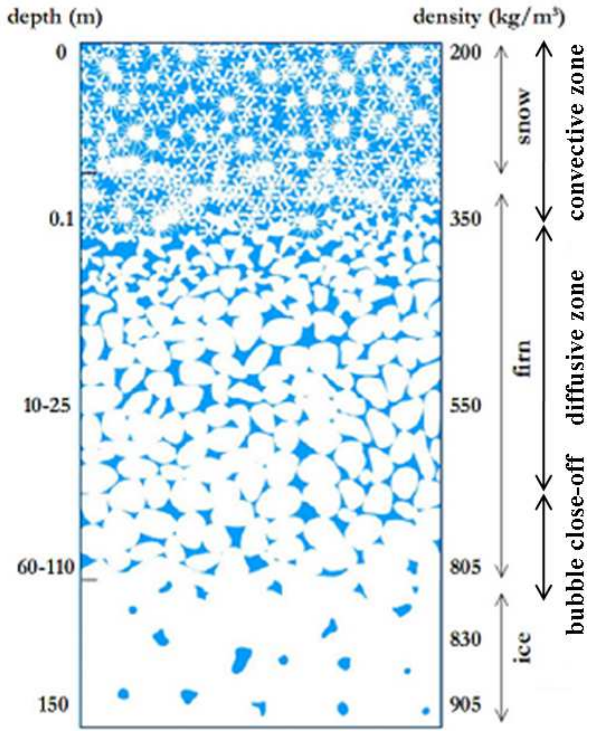

Figure 1. Polar firn structure as a function of depth and density. Scheme adapted from [5, 6].

The non-homogeneous transport of trace gases in firns can be modeled using the dynamic equations pro-

*The authors are with: [[1] Systems and Control Department, GIPSA-lab (UJF/CNRS), [2] Laboratoire de Glaciologie et Géophysique de l'Environnement (CNRS)] Université Joseph Fourier, 38 402 Saint Martin d'Héres, France. The corresponding author email is emmanuel.witrant@gipsa-lab.inpg.fr

posed in [7, 8], where a first approach for model validation and diffusion profiles identification based on firn air measurements is described. This approach was successfully used to describe the firn diffusion property for specific geographical locations, where the diffusivity profiles are sufficiently smooth, but cannot be generalized due to numerical instabilities in the identification process. Our aim is then to revise the modeling and identification algorithms using modern automatic control methodologies.

The transport model assumes a perfect gas, hydrostatic (pressure computation), isothermal firn, stationary flow (constant accumulation rate, temperature etc.), no thermal diffusion, no interaction (chemical, particles collision, gas transfer) between the gas and the pore walls. The following PDE model is then established (e.g. for a single gas) to describe the trace gas quantity in open pores $q(z,t)$ [7]:

$$\begin{cases} \partial_t q = D(z)\partial_{zz} q + \alpha(z)\partial_z q + \beta(z) q \\ q(0,t) = f(0)c_s(t) \doteq q_0(t) \\ k_1 \partial_z q(z_f,t) + k_2 q(z_f,t) = 0 \\ q(z,0) = q_I(z) \end{cases} \tag{1}$$

with the compact notation $\partial_x y \doteq \partial y / \partial x$ and:

$$\begin{aligned} \alpha(z) &\doteq \partial_z D(z) - D(z)\chi(z) - w(x) \\ \beta(z) &\doteq -D(z)\partial_z \chi(z) - \partial_z D(z)\chi(z) - \lambda \\ &\quad + \frac{v(x)\varepsilon(z)}{f(z)} \partial_z \left[\frac{f(z)}{\varepsilon(z)} \right] - \partial_z w(z) \end{aligned}$$

where $\chi(z) \doteq Mg/RT + f_z/f$, $q(z,t)$ is the trace gas quantity in open porosity, $D(z)$ is the diffusivity, λ is the radioactive decrease, M is the molar mass, $\varepsilon(z)$ the total porosity, $f(z)$ the open porosity, $v(z)$ the sinking speed of the layers, $w(z)$ the airflow speed in open porosity. The depth in the firn is determined by $0 \leq z \leq z_f$ and $c_s(t)$ is the atmospheric concentration of the trace gas. The mentioned physical variables are summarized in Table 1.

The model (1) writes in the compact form:

$$\begin{aligned} \partial_t q &= \partial_z \left[D \partial_z q - (D\chi + w) q \right] \\ &\quad + \left[-\lambda + v \left(\frac{\partial_z f}{f} - \frac{\partial_z \varepsilon}{\varepsilon} \right) \right] q \\ &= \partial_z \left[D(z)\partial_z q - V(z) q \right] + S(z) q \end{aligned}$$

which generally describes non-homogeneous transport in a variable-porosity medium, characterized by its diffusivity $D(z)$, an advection term $V(z)$ and a source term $S(z)$. It is related to (1) as $\alpha(z) = D_z(z) - V(z)$ and $\beta(z) = -V_z(z) + S(z)$.

In order to formulate the modeling and identification problems properly, we can distinguish between the chemical and physical parameters. The chemical variables (M, c_s, λ) depend on the gas considered while the physical parameters (f, w, v, ε, D) depend on the geographical locations and are measured or calculated for each firn. The atmospheric time-trend history $c_s(t)$ is reasonably well known for specific gas such as CO_2, CH_4, SF_6 and some halocarbons such as CH_3CCl_3. Such gases can then be used to determine the diffusive property of a firn D provided that some distributed (depth-dependent) measurement $q(z,t_f)$ is available. The simulations illustrating the different theoretical results correspond to the transport of CH_4 in *Dome C* (Dome Concordia or Dome Charlie, located in Antarctica at an altitude of 3,233 m above sea level), and presented in [3].

Notation	Physical variable
α_{accu}	site accumulation rate (m eq water$/yr$)
α_g	closed porosity
Δz	depth increment between model layers (m)
$\varepsilon(z)$	total porosity (pores vs. firn layer vol.)
ε_{co}	total porosity at close-off density level
$\rho(z)$	firn density versus depth (g/cm^3)
ρ_{ice}	density of pure ice (kg/m^3)
ρ_{co}	close-off density ($f/\varepsilon = 0.37$, g/cm^3)
c_{air}	air concentration
$f(z)$	open porosity (open pores vs. firn layer vol.)
g	acceleration of gravity ($m \cdot s^{-2}$)
M_{air}	molar mass of air (kg/mol)
q_{air}	air quantity in open pores
R	perfect gas constant ($J \cdot mol^{-1} \cdot K^{-1}$)
T	temperature (K)
$v(z)$	firn sinking speed due to snow accumulation
$w(z)$	advection speed compensating the air trapping in bubbles (m/yr)
z_f	total depth of the firn (m)
z_{co}	depth level at which there is no remaining open porosity (m)

Table 1. Main physical variables and notations

2. Optimal diffusivity identification

The diffusivity identification objective can be formulated as an optimization problem, where the diffusivity profile has to minimize the squared difference between the final concentration provided by the model and the measured one. The proposed approach is based on variational analysis applied to PDE optimization as described in [9]. More precisely, we extend some results presented in [10] for conservation laws to transport in a variable-porosity medium, following the proposed formalism. A detailed bibliography, convective conservation laws, shock waves and state nonlinearities are considered in [10].

2.1. Problem formulation

Our aim is to find the diffusivity profile D^* that minimizes the difference between the model output and the measurements. This corresponds to a final-cost optimization problem with dynamics (transport equations) and inequality constraints that writes as:

$$\min_D \mathscr{J}(D) = \mathscr{J}_{meas} + \mathscr{J}_{reg}$$
$$\text{under the constraints} \begin{cases} \mathscr{C}(q,D) = 0 \\ \mathscr{I}(D) < 0 \end{cases}$$

where $\mathscr{J}_{meas}$ denotes the cost associated with the measurements, $\mathscr{J}_{reg}$ is a regularization function, $\mathscr{C}(q,D)$ sets the dynamical constraint associated with the non-homogeneous transport model and $\mathscr{I}(D)$ corresponds to the inequality constraints determined from the physics on the optimized variable D. More specifically, the measurements cost is chosen as a weighted least-squares criterion and the equality constraints are included into the cost function $\mathscr{J}(D)$ by introducing the *Lagrange* or *Kühn and Türker* parameters λ_i. The inequality constraints can be introduced thanks to *Valentine*'s method or the barrier function proposed in [11] (chosen here). In the problem considered, the constraint $\mathscr{J}(D)$ is set on the diffusivity gradient, which necessitates a specific care that will be detailed later on. Considering the measurements of N gas, the resulting optimization problem is:

$$\min_D \mathscr{J}(D) \doteq \sum_{i=1}^{N} [\mathscr{J}_{meas}(q_i, q_{meas}) + \mathscr{J}_{trans}(\mathscr{C}(q_i,D))] + \mathscr{J}_{ineq}(D) + \mathscr{J}_{reg}(D) \quad (2)$$

with:

$$\begin{cases} \mathscr{J}_{meas} &= \frac{1}{2}\int_0^{z_f} r_i (q_{meas} - q_i|_{t=t_f})^2 \delta_z \, dz \\ \mathscr{J}_{trans} &= \int_0^{t_f}\int_0^{z_f} \lambda_i \mathscr{C}(q_i,D)\, dz dt \\ \mathscr{J}_{reg} &= \frac{1}{2}\int_0^{z_f} s(z) D^2 \, dz \end{cases}$$

where z_f and t_f are the final depth and time, respectively, $r_i(z) \geq 0$ and $s(z) > 0$ are user-defined tuning functions, $\delta_z(z)$ denotes the measurements location and $\mathscr{J}_{ineq}$ describes the inequality constraint. Our aim is to find the set of parameters $\{D, q_i, \lambda_i\}$ that minimizes the cost function $\mathscr{J}$. Note that the dependence of the cost in q_i could be removed from the fact that q_i depends on D through $\mathscr{C}$.

2.2. Linearized dynamics

In order to solve the previous optimization problem, the first step is to linearize the distributed dynamics and define an appropriate transport model. Consider the general transport equation

$$\begin{cases} \partial_t y + f_1(z,t)y + f_2(z,t)\partial_z y = \partial_z [g(y, \partial_z y, u)] \\ y(0,t) = y_0(t), \quad k_1 \partial_z y(L,t) + k_2 y(L,t) = 0 \\ y(z,0) = y_I(z) \end{cases} \quad (3)$$

Its linearized dynamics along the reference trajectory $(\bar{y}, \bar{u}, \bar{y}_I)$ with perturbations $(\tilde{y}, \tilde{u}, \tilde{y}_I)$ is given by

$$\begin{cases} \partial_t \tilde{y} + f_1(z,t)\tilde{y} + f_2(z,t)\partial_z \tilde{y} \\ \quad = \partial_z \left[\partial_y \bar{g}\, \tilde{y} + \partial_{\partial_z y} \bar{g}\, \partial_z \tilde{y} + \partial_u \bar{g}\, \tilde{u}\right] \\ \tilde{y}(0,t) = 0, \quad k_1 \partial_z \tilde{y}(L,t) + k_2 \tilde{y}(L,t) = 0 \\ \tilde{y}(z,0) = \tilde{y}_I(z) \end{cases} \quad (4)$$

where $\bar{g} \doteq g(\bar{y}, \partial_z \bar{y}, \bar{u})$.

Note that the particular choice of $\bar{y}(z,0) = y_I(z)$ directly implies that $\tilde{y}_I(z) = 0$, which may be a convenient condition in some applications. We can directly verify that $\tilde{u} = 0$ implies that $\tilde{y} = 0$.

The previous theorem applies directly to the general porosity model:

$$\begin{cases} \partial_t q = \partial_z [D(z)(\partial_z q - \chi(z) q) - w(z) q] + S(z) q \\ q(0,t) = q_{x=0}(t),\, k_1 \partial_z q(z_f,t) + k_2 q(z_f,t) = 0 \\ q(x,0) = q_I(x) \end{cases} \quad (5)$$

by considering the reference concentration $\bar{q}(x,t)$ satisfying (5). The linearized state $\tilde{q}$ resulting from a variation in the diffusivity profile $\tilde{D}$ then writes as:

$$\Sigma_{Lin} : \begin{cases} \partial_t \tilde{q} = \partial_z [\bar{D}(\partial_z \tilde{q} - \chi \tilde{q}) - w \tilde{q}] \\ \quad + \partial_z \left[(\partial_z \bar{q} - \chi \bar{q})\tilde{D}\right] + S\tilde{q} \\ \tilde{q}(0,t) = 0,\, k_1 \partial_z \tilde{q}(z_f,t) + k_2 \tilde{q}(z_f,t) = 0 \\ \tilde{q}(x,0) = \tilde{q}_I(x) \end{cases} \quad (6)$$

The linearized system is compared with the coupled dynamics on the test case as follows. A 5% variation on y_I induces a variation of the order of 4.5% on the normalized concentration profile but a negligible error (of the order 10^{-13}%, which corresponds to numerical noise) with the linearized model. This is related to the fact that the linear model obeys the same conservation law as the initial one. A 5% variation on D varies the normalized concentration profile by 1% (terminal value) while the normalized error associated with the linear model is less than 0.04%, as depicted in Figure 2. It can be noticed that the concentration error tends to accumulate at the bottom of the firn over time.

3. Adjoint state and gradient computation

3.1. Adjoint state

The proposed gradient computation implies to compute the adjoint state when the diffusivity variation

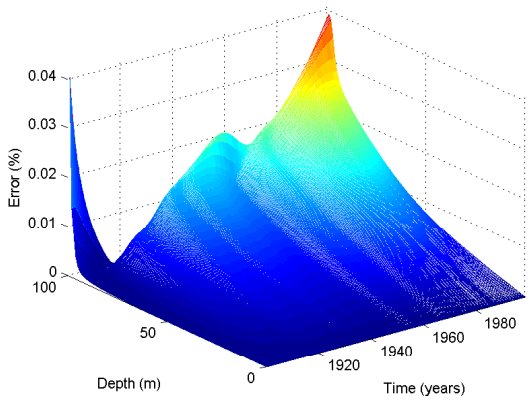

Figure 2. Linearization error for $\tilde{D} = 0.05\,D$.

is zero, e.g. $\tilde{D} = 0$. Such adjoint is given by the following theorem.

Theorem 3.1 *Consider the linearized transport equation without input:*

$$\begin{cases} \partial_t \tilde{y} = \partial_z \left[f_1(z,t)\partial_z \tilde{y} + f_2(z,t)\tilde{y} \right] + f_3(z,t)\tilde{y} \\ \tilde{y}(0,t) = 0, \quad k_1 \partial_z \tilde{y}(L,t) + k_2 \tilde{y}(L,t) = 0 \\ \tilde{y}(z,0) = 0 \end{cases}$$

The corresponding adjoint state is given as:

$$\begin{cases} \partial_t \lambda = -f_3 \lambda + (f_2 - \partial_z f_1)\,\partial_z \lambda - f_1 \partial_{zz} \lambda \\ \lambda(0,t) = 0, \\ f_1\, \partial_z \lambda + [f_1 k_2/k_1 - f_2]\lambda\,|_{z=L} = 0 \\ \lambda(z,T) = 0 \end{cases} \tag{7}$$

Proof 1 *The adjoint state equation is obtained as (integration by parts):*

$$\begin{aligned} &\int_0^T \int_0^L \lambda \left(\partial_t \tilde{y} - \partial_z \left[f_1 \partial_z \tilde{y} + f_2 \tilde{y} \right] - f_3 \tilde{y} \right) dz dt \\ &= \int_0^T \int_0^L \tilde{y} \left[-\partial_t \lambda - f_3 \lambda + (f_2 - \partial_z f_1)\,\partial_z \lambda - f_1 \partial_{zz} \lambda \right] dz dt \\ &\quad + \int_0^L \lambda \tilde{y} |_0^T dz - \int_0^T \left([f_1 \partial_z \tilde{y} + f_2 \tilde{y}]\,\lambda - f_1 \tilde{y}\, \partial_z \lambda \right) |_0^L dt \end{aligned}$$

All the components in the previous integrals are directly set to zero from (7) and by noticing that at $z = L$:

$$\begin{aligned} &[f_1 \partial_z \tilde{y} + f_2 \tilde{y}]\lambda - f_1 \tilde{y}\, \partial_z \lambda \\ &= [(-f_1 k_2/k_1 + f_2)\lambda - f_1\, \partial_z \lambda]\tilde{y} \end{aligned}$$

The adjoint state corresponding to the linearized system (6) without diffusivity variation is obtained thanks to the previous theorem by setting:

$$f_1 = \bar{D}, \quad f_2 = -(\bar{D}\chi + w), \quad f_3 = S,$$

and the adjoint state is:

$$\begin{cases} \partial_t \lambda = -S\lambda + (-w - \bar{D}\chi - \partial_z \bar{D})\,\partial_z \lambda - \bar{D}\partial_{zz} \lambda \\ \lambda(0,t) = 0, \\ \bar{D}\, \partial_z \lambda + [\bar{D} k_2/k_1 + (\bar{D}\chi + w)]\lambda\,|_{z=z_f} = 0 \\ \lambda(z,t_f) = 0 \end{cases} \tag{8}$$

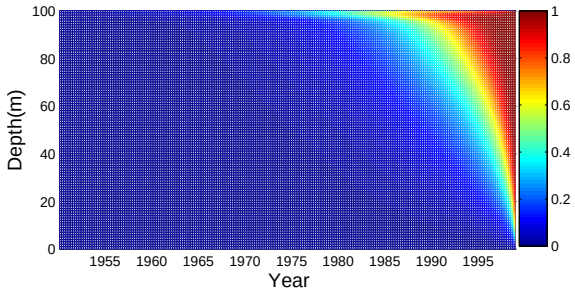

Figure 3. Adjoint state with $\lambda(z,t_f) = 1$.

The time and space evolution of the adjoint state for a unitary terminal condition ($\lambda(z,t_f) = 1$) is presented in Figure 3. We can note the impact of the depth on the step dispersion in the adjoint model. This is directly related to the depth dependency of the gas diffusion speed.

3.2. Inequality constraint

The fact that the inequality constraint applies on the diffusivity gradient as $\partial_z D < 0$ motivates the change of variables $\partial_z y_{IC} = u$ and $D = y_{IC}$ with $y_{IC}(z_f) = 0$ and where u is the new variable used for the optimization process. Introducing the associated *Lagrange* parameters $\lambda_{IC}(z,t)$ and a barrier function $\mathscr{R}(u)$, the cost is set with:

$$\begin{aligned} \mathscr{J}_{ineq} &= \int_0^L \lambda_{IC}(\partial_z y_{IC} - u) + \mathscr{R}(u)\, dz \\ &= \int_0^L -y_{IC}\partial_z \lambda_{IC} - u\lambda_{IC} + \mathscr{R}(u)\, dz + \lambda_{IC} y_{IC} |_0^{z_f} \end{aligned}$$

The fact that there is no dynamics involved is directly related to the algebraic nature of the constraint. The barrier function can be set as a log involving upper and lower bounds [11], or with the augmented Lagrangian [12].

3.3. Adjoint-based gradient

The last step to set the optimal diffusivity profile identification algorithm is to propose an adjoint-based gradient computation, based on the variational analysis. This is done thanks to the following theorem.

Theorem 3.2 *Consider the optimization problem (terminal cost, uncoupled states, input derivative constraint):*

$$\begin{aligned}\min_{u(z)} \mathscr{J} \doteq \sum_{i=1}^{N} \Big[\int_0^L \mathscr{P}(y_i(z,T))dz \\ + \int_0^T \int_0^L \lambda_i \mathscr{C}_i(y_i, y_{IC}, u) dz dt \Big] \\ + \int_0^L \lambda_{IC} \mathscr{C}_{IC}(y_{IC}, u) + \mathscr{R}(u) dz\end{aligned} \tag{9}$$

where $\mathscr{C}_i(y_i, y_{IC}, u)$ can be linearized as:

$$\begin{cases} \partial_t \tilde{y}_i = \partial_z [f_1(z,t)\partial_z \tilde{y}_i + f_2(z,t)\tilde{y}_i] \\ \qquad\qquad + f_3(z,t)\tilde{y}_i + \partial_z[f_4(z,t)\tilde{y}_{IC}] \\ \tilde{y}_i(0,t) = 0, \quad k_1 \partial_z \tilde{y}_i(L,t) + k_2 \tilde{y}_i(L,t) = 0 \\ \tilde{y}_i(z,0) = \tilde{y}_{Ii}(z) \end{cases}$$

and $\mathscr{C}_{IC}(y_{IC}, u) = \partial y_{IC} - u$ with $y_{IC}(z_f) = 0$.

The gradients of $\mathscr{J}$ with respect to the decision variables u and y_{Ii} along the reference trajectory $(\bar{u}, y(\bar{u}))$ are given by:

$$\nabla_u \mathscr{J} = \mathscr{R}'(\bar{u}) - \int_0^T \lambda_{IC}\, dt \tag{10}$$

$$\nabla_{y_{Ii}} \mathscr{J} = -\lambda_i(z,0) \tag{11}$$

where λ_i are the solutions of:

$$\begin{cases} \partial_t \lambda_i = -f_3 \lambda_i + (f_2 - \partial_z f_1)\partial_z \lambda_i - f_1 \partial_{zz} \lambda_i \\ \lambda_i(0,t) = 0, \\ k_1 f_1\, \partial_z \lambda_i + [k_2 f_1 - k_1 f_2]\lambda_i|_{z=L} = 0 \\ \lambda_i(z,T) = -\mathscr{P}'(\bar{y}_i(T)) \end{cases} \tag{12}$$

and λ_{IC} is obtained from:

$$\begin{cases} \partial_z \lambda_{IC} = \sum_{i=1}^{N} f_4 \partial_z \lambda_i \\ \lambda_{IC}(0,t) = 0, \end{cases} \tag{13}$$

Proof 2 *As we are interested in the gradient computation, achieved with a* sufficiently small *step, the analysis is established on the first order variation of the cost function around the reference trajectory $(\bar{y}, \bar{u})$ (defining y as the set $\{y_i, y_{IC}\}$), denoted as $\tilde{J}$. Considering the perturbation $(\tilde{y}, \tilde{u})$, we have:*

$$\begin{aligned}\tilde{\mathscr{J}}(\tilde{y}, \tilde{u}) \doteq \sum_{i=1}^{N} \Big\{ \int_0^L \mathscr{P}'(\bar{y}_i(z,T))\tilde{y}_i(z,T)\, dz \\ + \int_0^T \int_0^L \lambda\, [\partial_y \mathscr{C}(\bar{y}, \bar{u})\tilde{y} + \partial_u \mathscr{C}(\bar{y}, \bar{u})\tilde{u}]\, dz dt \Big\} \\ + \int_0^L \mathscr{R}'(\bar{u})\tilde{u}\, dz\end{aligned}$$

where $\lambda \doteq \{\lambda_i, \lambda_{IC}\}$, $\mathscr{C} \doteq \{\mathscr{C}_i, \mathscr{C}_{IC}\}$ and ∂_y involves the partial derivatives with respect to the derivatives of y (omitted to keep simple notations). This expression implies the linearized version of $\mathscr{C}(\cdot)$, obtained thanks to Section 2.2 as in (9). Applying integration by parts as in the proof of Theorem 3.1, the double-integral term involving y_i writes as:

$$\begin{aligned}\int_0^T \int_0^L \lambda_i [\partial_t \tilde{y}_i - \partial_z [f_1 \partial_z \tilde{y}_i + f_2 \tilde{y}_i] - f_3 \tilde{y}_i - \partial_z [f_4 \tilde{y}_{IC}]]\, dz dt \\ = \int_0^L \lambda_i \tilde{y}_i\, |_0^T dz - \int_0^T \int_0^L \lambda_i \partial_z [f_4 \tilde{y}_{IC}]\, dz dt\end{aligned}$$

where the last equality is obtained with (12). Introducing $\mathscr{J}_{ineq}$ as defined in Section 3.2, we have:

$$\begin{aligned}\int_0^T \int_0^L \lambda\, [\partial_y \mathscr{C}(\bar{y}, \bar{u})\tilde{y} + \partial_u \mathscr{C}(\bar{y}, \bar{u})\tilde{u}]\, dz dt - \int_0^L \lambda_i \tilde{y}_i\, |_0^T dz \\ = -\int_0^T \int_0^L \tilde{u} \lambda_{IC}\, dz dt\end{aligned}$$

where the successive simplifications are a direct consequence of (12)-(13) and the definition of y.

Introducing the previous equality in the expression of $\tilde{\mathscr{J}}$ and considering the solutions defined as in (12), it follows that:

$$\begin{aligned}\tilde{\mathscr{J}} = \int_0^L \Big[-\sum_{i=1}^{N} \lambda_i(z,0)\tilde{y}_{Ii}(z) \\ + \Big(\mathscr{R}'(\bar{u}) - \int_0^T \lambda_{IC}\, dt \Big) \tilde{u} \Big] dz\end{aligned}$$

where the fact that $\tilde{u}$ does not depend on time was used in the last equality. The gradients are finally obtained as in (10)-(11).

The optimization problem (2) fits within the previous formalism by noticing that:

$$\mathscr{P} = \frac{1}{2} r_i (q_{meas} - q_i|_{t=t_f})^2 \delta_z$$

$$\mathscr{R} = -\frac{1}{M} \log(-\partial_z D) + \frac{1}{2} s(z) \partial_z D^2$$

and considering the linearized dynamics (6). The gradients are then obtained thanks to Theorem 3.2 as (setting $\mathscr{I}(D) = \partial_z D$):

$$\nabla_{\partial_z D} \mathscr{J} = \frac{1}{M \partial_z D} + s \partial_z D - \int_0^T \lambda_{IC}\, dt \tag{14}$$

$$\nabla_{q_{Ii}} \mathscr{J} = -\lambda_i(z,0) \tag{15}$$

and (12) with:

$$f_1 = \bar{D},\ f_2 = -(\bar{D}\bar{\chi} + w),\ f_3 = S,\ f_4 = \partial_z \bar{q} - \bar{\chi}\bar{q},$$
$$\mathscr{P}' = -r_i (q_{meas} - q_i|_{t=t_f}) \delta_z$$

Considering the CH_4 experimental data, the gradient with respect to the input $\nabla_{\partial_z D}\mathscr{J}$ is obtained from the previous results and presented in Figure 4. It can be noticed that the algorithm converges smoothly within about 500 steps, which is very satisfying for this problem. Nevertheless, it is highly sensitive to the design weights and to the constraint, which will be the topic of future work.

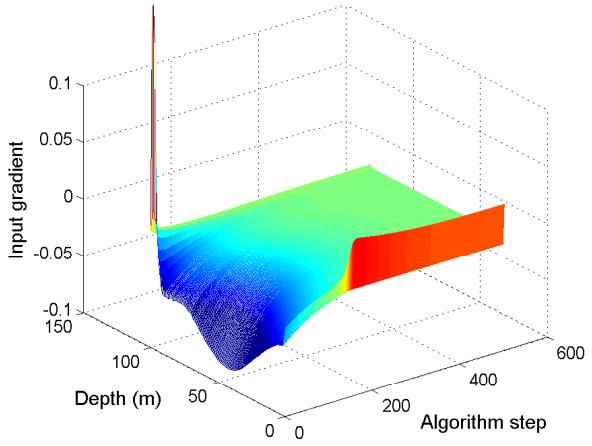

Figure 4. Algorithm convergence: evolution of the gradient $\nabla_{\partial_z D}\mathscr{J}$.

4. Conclusions

In this work, a new identification problem related to a challenging environmental application with high social impact has been presented: the diffusivity profile determination in firns based on trace gases measurements. This problem was formulated as an optimization problem involving distributed dynamics, a terminal cost constraint and an inequality constraint on the diffusivity gradient. Several new analytical results that apply generally to transport phenomena in variable-porosity media were derived, which allowed for a variational approach in the PDE framework. The optimal diffusivity profile was obtained thanks to an adjoint-based gradient-descent algorithm. The different results were illustrated and discussed on the basis of experimental measurements of CH_4 in *Dome C*.

5. Acknowledgements

The authors wish to thank Pr. Didier GEORGES for his fruitful remarks concerning the consideration of inequality constraints of the derivative type. This work was funded by CNRS program INSIS-PEPS-Automatique.

References

[1] IPCC, *Climate Change 2007: The Physical Science Basis. Contribution of Working Group I to the Fourth Assessment Report of the Intergovernmental Panel on Climate Change*, S. Solomon, D. Qin, M. Manning, Z. Chen, M. Marquis, K. Averyt, M. Tignor, and H. Miller, Eds. United Kingdom and New York, NY, USA: Cambridge University Press, 2007. [Online]. Available: http://www.ipcc.ch/ipccreports/assessments-reports.htm

[2] WMO, *Scientific Assessment of Ozone Depletion: 2006. Global Ozone Research and Monitoring Project - Report No.50*. Geneva: World Meteorological Organization, 2007. [Online]. Available: http://ozone.unep.org/Publications

[3] P. Martinerie, E. Nourtier-Mazauric, J.-M. Barnola, W. T. Sturges, D. R. Worton, E. Atlas, L. K. Gohar, K. P. Shine, and G. P. Brasseur, "Long-lived halocarbon trends and budgets from atmospheric chemistry modelling constrained with measurements in polar firn," *Atmospheric Chemistry and Physics*, vol. 9, pp. 3911–3934, 2009. [Online]. Available: http://www.atmos-chem-phys.net/9/3911/2009/

[4] J. Schwander, J.-M. Barnola, C. Andrie, M. Leuenberger, A. Ludin, D. Raynaud, and B. Stauffer, "The age of the air in the firn and ice at summit, greenland," *J. Geophys. Res.*, vol. 98, pp. 2831–2838, 1993.

[5] T. Sowers, M. Bender, D. Raynaud, and Y. Korotkevich, "δ^{15}N of N_2 in air trapped in polar ice: a tracer of gas transport in the firn and a possible constraint on ice age-gas age differences," *Journal of Geophysical Research*, vol. 97, pp. 15 683–15 697, 1992.

[6] A. Lourantou, "Contraindre l'augmentation en dioxyde de carbone (CO_2) lors des déglaciations basés sur son rapport isotopique stable du carbone ($\delta^{13}CO_2$)," Ph.D. dissertation, Université Joseph Fourier, 2008.

[7] V. Rommelaere, L. Arnaud, and J. Barnola, "Reconstructing recent atmospheric trace gas concentrations from polar firn and bubbly ice data by inverse methods," *Journal of Geophysical Research*, vol. 102, no. D25, pp. 30 069–30 083, 1997.

[8] V. Rommelaere, "Trois problèmes inverses en glaciologie," Ph.D. dissertation, Université Joseph Fourrier, Grenoble, France, 1997.

[9] J. Lions, *Optimal control of systems governed by partial differential equations*. Springer, 1971.

[10] D. Jacquet, "Macroscopic freeway modelling and control," Ph.D. dissertation, Institut National Polytechnique de Grenoble, 2006.

[11] S. Boyd and L. Vandenberghe, *Convex Optimization*. Cambridge University Press, 2004.

[12] G. Cohen and D. Zhu, *Advances in Large Scale Systems*. Greenwich, Connecticut: JAI Press, 1984, vol. I, ch. Decomposition coordination methods in large scale optimization problems. The nondifferentiable case and the use of augmented Lagrangians, pp. 203–266.